



Thermal and chemical variations in subcrustal cratonic lithosphere: evidence from crustal isostasy

Walter D. Mooney^{a,*}, John E. Vidale^b

^a*Earth Quake Hazards Team, United States Geological Survey, MS 977, 345 Middlefield Road, Menlo Park, CA 94025, USA*

^b*Earth and Space Sciences Department, UCLA, Los Angeles, CA 90095-1567, USA*

Abstract

The Earth's topography at short wavelengths results from active tectonic processes, whereas at long wavelengths it is largely determined by isostatic adjustment for the density and thickness of the crust. Using a global crustal model, we estimate the long-wavelength topography that is not due to crustal isostasy. Our most important finding is that cratons are generally depressed by 300 to 1500 m in comparison with predictions from pure crustal isostasy. We conclude that either: (1) cratonic roots may be 50 to 300 °C colder than previously suggested by thermal models, or (2) cratonic roots may be, on average, less depleted than suggested by studies of shallow mantle xenoliths. Alternatively, (3) some combination of these conditions may exist. The thermal explanation is consistent with recent geothermal studies that indicate low cratonic temperatures, as well as seismic studies that show very low seismic attenuation at long periods (150 s) beneath cratons. The petrologic explanation is consistent with recent studies of deep (>140 km) mantle xenoliths from the Kaapvaal and Slave cratons that show 1–2% higher densities compared with shallow (<140 km), highly depleted xenoliths.

© 2003 Elsevier B.V. All rights reserved.

Keywords: Isostasy; Crustal structure; Cratons; Xenoliths

1. Introduction

The long-wavelength topography of the Earth's surface is generally due to variations in crustal thickness, in combination with the large density contrast between crust and mantle (Turcotte and Schubert, 1982; Schubert et al., 2001; Watts, 2001). Topography can also be supported by the flexural rigidity of the lithosphere, but only on length scales much shorter than we investigate here. Topography that is not compensated by the crust is compensated by lateral

density contrasts below the crust. Here, we take advantage of recent improvements in our understanding of crustal structure to look deeper, at the lithosphere below the crust. The essence of our analysis is to make an isostatic correction for the known crustal part of the lithosphere to reveal the part of the topography that can only result from lateral density variations below the crust. Local dynamic uplifts associated with mantle convection, and mantle plumes in particular, may be important in some regions, but are not modeled in this global study.

Lateral density contrasts in the lithosphere arise from variations in both composition and temperature. The small magnitude of topographic and geoid anomalies, coupled with geochemical evidence, has

* Corresponding author. Tel.: +1-650-329-4764; fax: +1-650-329-5163.

E-mail address: mooney@usgs.gov (W.D. Mooney).

led to the recognition that the uppermost mantle beneath continents is likely to be colder, but of lighter composition than mantle beneath oceans (Jordan, 1975; Boyd, 1989). The isopicnic hypothesis states that these two effects nearly cancel, leaving only small lateral differences in density (Jordan, 1978). In this paper we show that cratons are generally depressed by about 300 to 1500 m in comparison with predictions from pure crustal isostasy. We interpret this observation in terms of excess density within craton roots, either due to colder temperatures or less chemical depletion, or both (cf. Kaban et al., 2003).

2. Data and analysis

We use ETOPO5 (National Geophysical Data Center, 1993), which consists of the Earth's surface elevation averaged over a 5 min grid, filtered as shown in Fig. 1a. The same filter is applied to all the data presented in this paper. This degree of smoothing removes the short-wavelength uncompensated topography that results from the elastic strength of the lithosphere, and emphasizes the long-wavelength patterns of uncompensated topography. Thus, we model lithospheric properties at wavelengths comparable to models derived from global surface wave tomography (i.e., >2000 km).

The signature of the crust, which is the upper 5 to 80 km of the Earth, must be removed to reveal subcrustal anomalies. Lateral variations in crustal thickness and density dominate the topography. For example, the high Andes and the Tibetan plateau are buoyed by the thickest crust, whereas the low-lying oceans have the thinnest crust. We use the global model Crust 5.1 (Mooney et al., 1998), which is based on measurements of crustal thickness and seismic velocity from seismic refraction experiments, and densities from laboratory studies (Christensen and Mooney, 1995). Where refraction data are not available, the model extrapolates based on tectonic affinity.

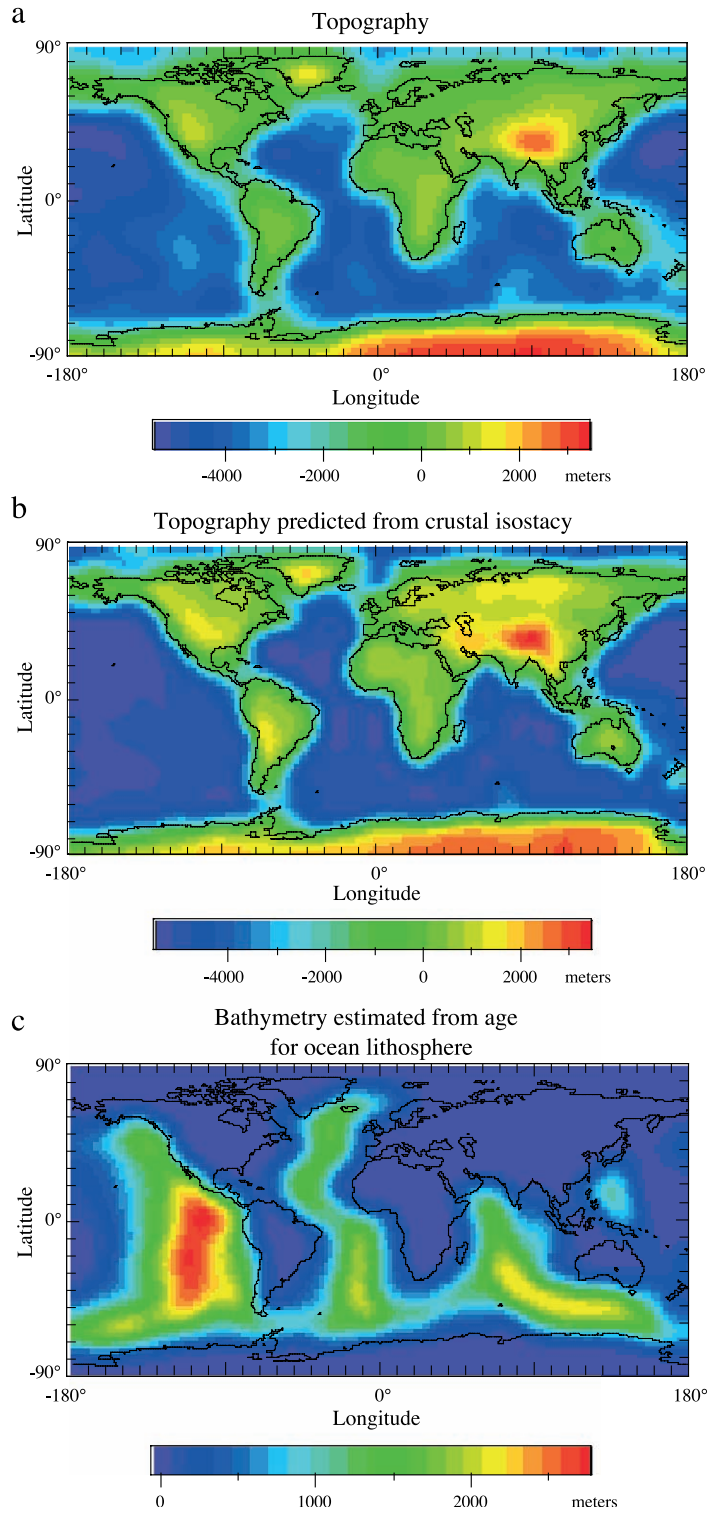
In order to avoid model artifacts, we emphasize only the conclusions that are derived from the regions of the densest refraction coverage.

Previous attempts to model the Earth's topography differ from this study in the following respects: (1) LeStunff and Ricard (1995) and Simons and Hager (1997) used less comprehensive models of crustal structure; (2) Forte (1995) and Forte et al. (1993) divided the Earth into oceanic and continental regions, each with an average ocean or continent structure and (3) Pari and Peltier (1996) defined cratons from seismic tomography maps rather than geologic maps, as is done here. Studies that focus on shorter-wavelength structure often use gravity data (Pari and Peltier, 1996; Simons and Hager, 1997). Other studies have focused on the properties of the deep mantle (Forte and Mitrovica, 2001). The approach taken in our study is most similar to that of Forte and Perry (2000); however, they also use global seismic tomographic models to infer density variations in the mantle. We do not model the geoid here because lower mantle density variations cause larger geoid signals than lithospheric density variations (Simons and Hager, 1997).

The topography estimated from Crust 5.1 is shown in Fig. 1b. Airy compensation is assumed at the base of the crust, with a constant mantle density of 3350 kg/m³ (Dziewonski and Anderson, 1981). In other words, when calculating pure crustal isostasy, the crust in each cell is assumed to float isostatically on the upper mantle (Turcotte and Schubert, 1982).

The sinking that accompanies the cooling of oceanic crust with age is well known from the observation that mid-ocean ridges stand significantly higher than the old ocean floor. This topography has been explained by a half-space model of a lithosphere that cools by conduction (Parsons and Sclater, 1977). The topography predicted by the age of the seafloor, as derived from magnetic anomalies (Mueller et al., 1993), is shown in Fig. 1c, with zero depth assigned to 150 Ma ocean floor. There are alternative models for the dependence of topography on seafloor age that

Fig. 1. (a) The topography of the Earth. ETOPO5 (National Geophysical Data Center, 1993) is averaged over 5° by 5° cells. This and the following figures are resampled by bilinear interpolation to 2.5° by 2.5° cells, then smoothed by five convolutions with a 7.5° by 7.5° boxcar function. The result is that only long-wavelength features are resolved. (b) Topography predicted by Crust 5.1 (Mooney et al., 1998) floating on mantle with density 3350 kg/m³. (c) Topography predicted by a half space model of cooling oceanic lithosphere (Parsons and Sclater, 1977). Note that 150 Ma oceanic crust is arbitrarily assigned zero topography.



correct for inferred dynamic topography and/or assume plate rather than halfspace cooling models (e.g., Stein and Stein, 1996), but our conclusions for cratonic lithosphere do not depend on our choice of an oceanic cooling model. Thermal perturbations from hotspots are not taken into account in our modeling, and the anomalies that appear to be due to these features are identified below.

3. Uncertainties

Topography (Fig. 1b) due to crustal isostasy depends upon crustal thickness and density. Crustal thickness is accurate to ± 2 km beneath a modern, reversed refraction line. The uncertainty in average crustal thickness across 5° by 5° blocks is difficult to quantify, but we estimate that it is ± 3 km in regions with seismic refraction profiles and ± 7 km in regions for which crustal structure is extrapolated (Mooney et al., 1998; 2002). However, the multi-cell smoothed values in all our figures average out much of the variation from cell to cell, so we subjectively estimate that the long-wavelength crustal thickness is accurate to ± 2 km in regions with seismic refraction profiles and ± 4 km in regions for which crustal structure is extrapolated. A comparison of our smoothed crustal thickness with published contour maps of crustal thickness for North America, Europe, and the former USSR support these estimates (Mooney and Braile, 1989; Meissner et al., 1987; Belousov et al., 1991). There is an average uncertainty of ± 0.035 kg/m³ in estimating density from compressional-wave seismic velocity (Christensen and Mooney, 1995).

Topography due to crustal isostasy is best determined in North America, Eurasia, and Australia (Fig. 1d). In these well-studied areas, the uncertainty in the smoothed model topography (Fig. 1b) is 200 m. The crustal structure in Africa, Greenland, and South America, in contrast, is largely extrapolated from areas with similar geology. Using the estimated uncertainties, the

predicted topography in these extrapolated regions may be accurate to within 400 m. In view of this variability in model uncertainty, we base our conclusions only on results for well-studied areas, and include other regions for completeness and for comparison with previous work (e.g., Forte and Perry, 2000).

4. Results

Fig. 2a shows the residual topography that is not compensated by the crustal part of the continental lithosphere or the cooling of oceanic plates (cf. Kaban et al., 1999). The residual topography is approximately equal to actual topography (Fig. 1a) with the corrections for crustal structure (Fig. 1b) and cooling oceanic lithosphere (Fig. 1c) subtracted. (A correction is needed because the oldest oceanic floor was assigned zero depth in Fig. 1c, rather than the actual average bathymetry of 150 Ma crust.)

Three regions in Fig. 2a have been filled with zeroes prior to smoothing. (1) The Ross Ice Sheet, on the edge of Antarctica south of New Zealand, was given zero elevation in ETOPO5, rather than the true ocean depth. (2) Near the North Pole, our ocean age model did not have ages for crust in several ocean basins. Both of these unknowns result in several km of apparent topography that cannot be interpreted, so these small regions are set to zero. (3) The area in the southwest Pacific extending from the east coast of Australia to about Tonga is also set to zero because it also is not dated in the ocean age model. This area contains numerous plateaus and back-arc basins of uncertain crustal thickness, as well as several subduction zones.

Fig. 2b shows a recent map of variations in seismic shear velocity from 100 to 175 km depth (Grand et al., 1997), and Fig. 2c is a highly smoothed map of the distribution of cratons that has been filtered in the same manner as the geophysical maps (Fig. 2a and b). The well-known correlation of high seismic velocities with cratons, and low seismic velocities with young

Fig. 2. (a) Residual topography unexplained by pure crustal isostasy and the cooling plate oceanic lithosphere model (Fig. 1c). (b) Shear wave velocity variation between 100- and 175-km depths (Grand et al., 1997). The map is obtained by inversion of seismic body waves (Grand and Helmberger, 1984). (c) Highly smoothed map of the cratons (Mooney et al., 1998). All Archean and Proterozoic shields and platforms are considered cratons. The initial, unsmoothed map agrees well with a recent compilation (Goodwin, 1996). (d) Distribution of the refraction profiles on which the model Crust 5.1 is based. Darker areas have denser coverage, and therefore the crustal structure is better resolved than in lighter areas.

oceanic crust, is evident (e.g., Polet and Anderson, 1995). Cratonic regions are generally depressed 300 to 1500 m. Cratons where refraction data are available to constrain crustal properties (Fig. 1d) appear, in general, more depressed. Large parts of Eurasia, South America, and the cratonic part of North America are depressed by 600 to 1500 m. Australia and west Africa are only depressed by about 300 m. Several continent regions, including western North America, southern Africa, western Europe, Greenland and eastern Asia show little anomalous topography. Most tectonically active regions are in this category. Thus, when compared with pure crustal isostasy, many cratons show depressed topography, as well as high lithospheric shear wave velocities, suggesting the presence of cold, dense cratonic roots.

Changing the two most loosely constrained features of our model, (1) making the reference age of the oceanic crust younger than 150 My, or (2) assuming a plate rather than halfspace cooling model for oceanic lithosphere, would enhance the depression of the cratonic regions. A region with abundant refraction control, the cratons comprising northern Eurasia including the Caspian Sea and the Urals, is strongly depressed. The crust of the Ural mountains is well studied; this lack of compensation has been noticed in local studies (Artemjev et al., 1994; Yegorova et al., 1995) and is visible in a similar study (LeStunff and Ricard, 1995). It is clear that the crust of northern Eurasia is underlain by denser-than-average mantle lithosphere. This region is composed of Archean and Proterozoic crustal terranes (Goodwin, 1996).

In several well-constrained areas, the ocean floor is higher than predicted by our model. Iceland is the most prominent anomaly, but the Indian and Pacific Ocean hotspots with the highest buoyancy flux (Sleep, 1990) are also elevated by 300 m. Deeper mantle buoyancy forces may account for the Pacific and Indian ocean topographic anomalies, since these hotspots appear in older crust (Sandwell and MacKenzie, 1989). Many other hotspots and plateaus also correspond with topographic highs. The positive topographic anomaly associated with Iceland requires a subcrustal low-density anomaly (i.e., positive buoyancy). Our model already corrects for the thermal structure of young oceanic lithosphere, but the region surrounding Iceland still stands 500 to 1000 m higher than predicted. Although the hotspot buoyancy flux under Iceland is

estimated to be less than that of other hotspots (Sleep, 1990), Iceland appears to be surrounded by the largest subcrustal density deficit. This has been noted in local studies (Smallwood et al., 1995; White et al., 1995). Hot mantle has been inferred to persist as deep as 660 km beneath Iceland (Shen et al., 1998; Wolfe et al., 1997; Foulger et al., 2000).

5. Discussion

The analysis of mantle xenoliths found in kimberlites shows that cratonic mantle is colder and more chemically depleted than oceanic mantle (Finnerty and Boyd, 1987; Boyd, 1989). The mantle beneath cratons has been estimated to be approximately 200° colder on average than the mantle beneath mature ocean basins in the depth range from 40 to 200 km (Jordan, 1988). However, the composition of mantle xenoliths also suggests that the uppermost mantle is roughly 1% less dense under cratons than under non-cratonic crust (Boyd and McCallister, 1976). Thus, purely thermal effects would cause 1 km of depression of cratons, while chemical depletion would cause 1 km of uplift (Jordan, 1988).

The observed depression of cratons in Fig. 2a indicates that cratonic roots are denser than non-cratonic upper mantle. Therefore, the cratonic roots are either colder or less depleted than is suggested by the isopicnic hypothesis (Jordan, 1978; 1988). The observed average value of 500 m of depression of cratons can be explained by 100 °C colder temperatures in the cratonic roots or, alternatively, by 0.7% depletion, rather than 1% depletion. A combination of these explanations is also a viable possibility. The thermal explanation is consistent with a recent global study of the thermal regime of continental lithosphere (Artemieva and Mooney, 2001) that shows temperature differences of as much as 500 °C between cratonic and Phanerozoic upper mantle at a depth of 150 km. The thermal explanation is also consistent with the very low seismic attenuation that correlates with cratons (Billien et al., 2000).

Conversely, the petrologic explanation for topographic depression of cratons is consistent with recently reported data from mantle xenoliths from the Kaapvaal (southern Africa) and Slave (northwest Canada) cratons that indicate less chemical depletion

in deep lithospheric roots. Boyd et al. (1999) report densities for Kaapvaal garnet lherzolites, and shows that the deeper (>140 km), high-temperature samples are 1–2% denser than the highly depleted samples from shallower (<140 km) depth. In accord with Boyd et al. (1999), xenolith samples from the Slave craton indicate that the lithosphere is layered, with a denser, more iron-rich layer below 145 km (Griffin et al., 1999). Thus, evidence from the Kaavaal and Slave cratons points to dense lithospheric roots below 140 km. These observations suggest that the magnitude of negative lithospheric buoyancy is proportional to the thickness of the lithospheric root below 140 km.

Dense cratonic roots, such as we infer, are consistent with observed geoid anomalies only if restricted to roughly the upper 100–250 km of the subcrustal lithosphere. The geoid, whose variations have an amplitude of about 100 m, is dominated by the effects of slabs, hotspots, and glacial rebound (Simons and Hager, 1997). The average geoid low over platforms and shields has been estimated to be only 5 to 10 m (LeStunff and Ricard, 1995; Shapiro et al., 1999). Compensation at 100-km depth of 1 km of depressed topography would produce a 10 m geoid low (Haxby and Turcotte, 1978).

Our model of dense cratonic roots differs from previous estimates of density variation in the subcrustal lithosphere. The model of Jordan (1988) has no density contrast between cratonic and non-cratonic lithosphere. The model of LeStunff and Ricard (1995), based on geoid and topography modeling, indicates different density variations below the crust, although similar anomalous topography is observed. Mantle convection modeling of the geoid and gravity also suggests that there is excess density beneath cratons, but that it is deep-seated and descending with mantle convection (Pari and Peltier, 1996; Pari, 2001).

Part of the residual topography in Fig. 2a may be due to the density variations deep in the mantle that drive mantle convection (Forte and Perry, 2000). For example, Africa has the only large craton that is not depressed in Fig. 2a. The low shear velocities at the base of the mantle beneath Africa (Woodhouse and Dziewonski, 1984) may be due to a low-density structure that can elevate Africa by more than a kilometer (Lithgow-Bertelloni and Silver, 1998). This anomalous elevation of Africa has been previously noted from bathymetric data (Nyblade and Robinson,

1994). Further crustal data are needed to evaluate our African results because there is little control on crustal thickness and density (Fig. 1d).

We may compare our map with predictions of topography calculated from estimates of mantle density variations based on the history of subduction in the past few hundred million years and the Earth's geoid anomaly (Ricard et al., 1993; Lithgow-Bertelloni and Richards, 1995). Such modeling of the geoid and topography predicts that subduction at the western edge of the Americas and along the western margin of the Pacific would produce up to 1 km of depressed topography. Our estimates of residual topography, however, are significantly smaller in amplitude and more localized than the predictions of flow modeling of the geoid.

It has been noted that whole-mantle models of circulation could explain the dynamic surface topography data if there is a large downward increase in viscosity (by a factor of 50 or more) across the 660 km seismic discontinuity (Pari, 2001). Pari (2001) also noted that a perfectly layered model of the circulation led to accurate descriptions of the long-wavelength dynamic surface topography constraints. Forte and Mitrovica (2001) argue for a high-viscosity layer near a depth of 2000 km by modeling surface topography, gravity, and plate velocity data. Radial variations in viscosity may also be important in the uppermost mantle: thick cratonic roots appear to encounter higher viscosity, with basal drag slowing plate motion (Stoddard and Abbott, 1996; Artemieva and Mooney, 2002). Thus, deep lithospheric roots appear to play an important role in determining both surface topography and the velocity of plate motions.

6. Conclusions

We have used a recent global crustal model to calculate crustal isostasy, which we compare with observed topography, upper mantle shear-wave tomography maps, and the global distribution of cratonic crust. The calculation of crustal isostasy is most reliable for those regions of the Earth with good seismic control on crustal structure (North America, Eurasia, Australia, and oceanic regions), and we base our conclusions on those regions. After subtracting pure crustal isostasy from observed topography, we

find that cratons are generally depressed by about 300 to 1500 m due to negative buoyancy (excess density) in the sub-crustal lithosphere (cf. Kaban et al., 2003). This negative buoyancy may be due to either: (1) lithospheric temperatures that are about 100 °C colder than is commonly assumed, or (2) a lesser degree of chemical depletion (approximately 0.7% vs. 1.0%) in cratonic lithosphere. Combinations of these two factors will also satisfy our observations. The thermal explanation is consistent with high seismic velocities and very low seismic attenuation in cratonic lithosphere. The petrologic explanation is consistent with recent studies of xenoliths from the Kaapvaal and Slave cratons that indicate that the density of the lithosphere increases 1–2% below 140 km. The petrologic explanation of our results also implies that the deeper a cratonic root extends below 140 km, the greater the negative buoyancy, and the larger the topographic depression.

Acknowledgements

This study was made possible by the provision of data and models from Steve Grand, Gabi Laske, Guy Masters, Carolina Lithgow-Bertelloni, David Sandwell, and William Moore. Discussions with Thomas Jordan, Art Lachenbruch, Misha Kaban, Wayne Thatcher, Yu-Shen Zhang, Brad Hager, Irina Artemieva, Paul Tackley, and the late Ron Girdler are appreciated. Irina Artemieva, Wouter Bleeker, Walter R. Roest, and Alan Jones provided reviews that significantly improved the text.

References

- Artemieva, I.M., Mooney, W.D., 2001. Thermal thickness and evolution of Precambrian lithosphere: a global study. *J. Geophys. Res.* 106, 16387–16414.
- Artemieva, I.M., Mooney, W.D., 2002. On the relations between cratonic lithosphere thickness, plate motions, and basal drag. *Tectonophysics* 358, 211–231.
- Artemjev, M.E., Kaban, M.K., Kucherinenko, V.A., Demyanov, G.V., Taranov, V.A., 1994. Subcrustal density inhomogeneities of Northern Eurasia as derived from the gravity data and isostatic models of the lithosphere. *Tectonophysics* 240, 249–280.
- Belousov, V.V., Pavlenkova, N.I., Egorkin, A.V., 1991. Deep Structure of the Territory of the USSR Nauka, Moscow. 224 pp.
- Billien, M., Leveque, J.-J., Trampert, J., 2000. Global maps of Rayleigh wave attenuation for periods between 40 and 150 seconds. *Geophys. Res. Lett.* 27, 3619–3622.
- Boyd, F.R., 1989. Compositional distinction between oceanic and cratonic lithosphere. *Earth Planet. Inter.* 96, 15–26.
- Boyd, F.R., McCallister, R.H., 1976. Densities of fertile and sterile garnet peridotites. *Geophys. Res. Lett.* 3, 509–512.
- Boyd, F.R., Pearson, D.G., Mertzman, S.A., 1999. Spinel-facies peridotites from the Kaapvaal root. In: Gurney, J.J., Gurney, J.L., Pascoe, M.D., Richardson, S.H. (Eds.), *Proceedings of the VII International Kimberlite Conference*. Red Roof Design, Cape Town, pp. 40–48.
- Christensen, N.I., Mooney, W.D., 1995. Seismic velocity structure and composition of the continental crust. *J. Geophys. Res.* 100, 9761–9788.
- Dziewonski, A.M., Anderson, D.L., 1981. Preliminary reference Earth model. *Phys. Earth Planet. Inter.* 25, 297–356.
- Finnerty, A.A., Boyd, F.R., 1987. Thermobarometry for garnet peridotites: basis for the determination of thermal and compositional structure of the upper mantle. In: Nixon, P.H. (Ed.), *Mantle Xenoliths*. Wiley, Chichester, pp. 381–402.
- Forte, A.M., 1995. Continent ocean chemical heterogeneity in the mantle based on seismic tomography. *Science* 268, 789.
- Forte, A.M., Mitrovica, J.X., 2001. Deep-mantle high-viscosity flow and thermochemical structure inferred from seismic and geodynamic data. *Nature* 410, 1049–1056.
- Forte, A.M., Perry, H.K.C., 2000. Geodynamic evidence for a chemically depleted continental tectosphere. *Science* 290, 1940–1944.
- Forte, A.M., Peltier, W.R., Dziewonski, A.M., Woodward, R.L., 1993. Dynamic surface topography—a new interpretation based upon mantle flow derived from seismic tomography. *Geophys. Res. Lett.* 20, 225–228.
- Foulger, G., 2000. The seismic anomaly beneath Iceland extends down to the mantle transition zone and no deeper. *Geophys. J. Int.* 142, F2–F5.
- Goodwin, A.M., 1996. *Principles of Precambrian Geology*. Academic Press, San Diego. 327 pp.
- Grand, S.P., Helmberger, D.V., 1984. Upper mantle shear structure of North America. *Geophys. J. R. Astron. Soc.* 76, 399–438.
- Grand, S.P., vanderHilst, R., Widiyantoro, S., 1997. Global seismic tomography: a snapshot of convection in the Earth. *GSA Today* 7, 1–7.
- Griffin, W.L., Doyle, B.J., Ryan, C.G., Pearson, N.J., O'Reilly, S.Y., Davies, R., Kivi, K., Van Achterbergh, E., Natapov, L.M., 1999. Layered mantle lithosphere in the Lac de Gras, Slave Craton: composition, structure and origin. *J. Petrol.* 40, 705–727.
- Haxby, W.F., Turcotte, D.L., 1978. On isostatic geoid anomalies. *J. Geophys. Res.* 83, 5473–5478.
- Jordan, T.H., 1975. The continental tectosphere. *Rev. Geophys.* 13, 1–12.
- Jordan, T.H., 1978. Composition and development of continental tectosphere. *Nature* 274, 544–548.
- Jordan, T.H., 1988. Structure and formation of continental tectosphere. *J. Petrol.*, 11–37.
- Kaban, M.K., Schwintzer, P., Tikhotsky, S.A., 1999. A global

- isostatic gravity model of the Earth. *Geophys. J. Int.* 136, 519–538.
- Kaban, M.K., Schwintzer, P., Artemieva, I.M., Mooney, W.D., 2003. Density of the continental roots: compositional and thermal contributions. *Earth Planet. Sci. Lett.* 209, 53–69.
- LeStunff, Y., Ricard, Y., 1995. Topography and geoid due to lithospheric mass anomalies. *Geophys. J. Int.* 122, 982–990.
- Lithgow-Bertelloni, C., Richards, M.A., 1995. Cenozoic plate driving forces. *Geophys. Res. Lett.* 22, 1317–1320.
- Lithgow-Bertelloni, C., Silver, P.G., 1998. Dynamic topography, plate driving forces and the African superswell. *Nature* 395, 269–272.
- Meissner, R., Wever, T., Flueh, E.R., 1987. The Moho in Europe—implications for crustal development. *Ann. Geophys., Ser. B* 5, 357–364.
- Mooney, W.D., Braile, L.W., 1989. The seismic structure of the continental crust and upper mantle of North America. In: Bally, A.W., Palmer, A.R. (Eds.), *The Geology of North America—An overview*. Geological Society of America, Boulder, CO, pp. 39–52.
- Mooney, W.D., Laske, G., Masters, T.G., 1998. Crust 5.1: a global crustal model at $5^\circ \times 5^\circ$. *J. Geophys. Res.* 103, 727–748.
- Mooney, W.D., Prodehl, C., Pavlenkova, N.I., 2002. Seismic velocity structure of the continental lithosphere from controlled source data. In: Lee, W.H.K., Kanamori, H., Jennings, P.C., Kisslinger, C. (Eds.), *International Handbook of Earthquake and Engineering Seismology*, vol. 81A. Academic Press, San Diego, CA, pp. 887–910.
- Mueller, R.D., Roest, W.R., Royer, J.-Y., Gahagan, L.M., Sclater, J.G., 1993. A digital age map of the ocean floor.
- Nyblade, A.A., Robinson, S.W., 1994. The African Superswell. *Geophys. Res. Lett.* 21, 765–768.
- Pari, G., 2001. Crust 5.1-based inference of the Earth's dynamic surface topography: geodynamic implications. *Geophys. J. Int.* 144, 501–516.
- Pari, G., Peltier, W.R., 1996. The free-air gravity constraint on subcontinental mantle dynamics. *J. Geophys. Res.* 101, 28105–28132.
- Parsons, B., Sclater, J.G., 1977. An analysis of ocean floor bathymetry and heat flow with age. *J. Geophys. Res.* 82, 803–827.
- Polet, J., Anderson, D.L., 1995. Depth extent of cratons as inferred from tomographic studies. *Geology* 23, 205–208.
- Ricard, Y., Richards, M.A., Lithgow-Bertelloni, C., LeStunff, Y., 1993. A geodynamic model of mantle density heterogeneity. *J. Geophys. Res.* 98, 21895–21909.
- Sandwell, D.T., MacKenzie, K.R., 1989. Geoid height versus topography for oceanic plateaus and swells. *J. Geophys. Res.* 94, 7403–7418.
- Schubert, G., Turcotte, D.L., Olsen, P., 2001. *Mantle Convection in the Earth and Planets*. Cambridge Univ. Press, Cambridge, UK. 940 pp.
- Shapiro, S.S., Hager, B.H., Jordan, T.H., 1999. Stability and dynamics of the continental tectosphere, in composition, deep structure, and evolution of continents. In: van der Hilst, R.D., McDonough, W.F. (Eds.), *Lithos* 48, pp. 115–133.
- Shen, Y., Solomon, S.C., Bjarnason, I.T., Wolfe, C.J., 1998. Seismic evidence for lower mantle origin of the Iceland plume. *Nature* 395, 62–65.
- Simons, M., Hager, B.H., 1997. Localization of the gravity field and the signature of glacial rebound. *Nature* 390, 500–504.
- Sleep, N.H., 1990. Hotspots and mantle plumes: some phenomenology. *J. Geophys. Res.* 95, 6715–6736.
- Smallwood, J.R., White, R.S., Minshull, T.A., 1995. Sea-floor spreading in the presence of the Iceland plume: the structure of the Reykjanes Ridge at $61^\circ 40' N$. *J. Geol. Soc. (Lond.)* 152, 1023–1029.
- Stein, S., Stein, C.A., 1996. Thermo-mechanical evolution of oceanic lithosphere: Implication for the subduction process and deep earthquakes. In: Bebout, G.E., Scholl, D.W., Kirby, S.H., Platt, J.P. (Eds.), *In Subduction: Top to Bottom*. Geophysical Monograph, vol. 96. American Geophysical Union, Washington, pp. 1–17.
- Stoddard, P.R., Abbott, D., 1996. Influence of the tectosphere upon plate motion. *J. Geophys. Res.* 101, 5425–5433.
- Turcotte, D.L., Schubert, G., 1982. *Geodynamics; Applications of Continuum Physics to Geological Problems*. Wiley, New York. 450 pp.
- Watts, A.B., 2001. *Isostasy and Flexure of the Lithosphere*. Cambridge Univ. Press, Cambridge, UK. 458 pp.
- White, R.S., Brown, J.W., Smallwood, J.R., 1995. The temperature of the Iceland plume and origin of outward-propagating V-shaped ridges. *J. Geol. Soc. (Lond.)* 152, 1039–1045.
- Wolfe, C.J., Bjarnason, I.T., Vandercar, J.C., Solomon, S.C., 1997. Seismic structure of the Iceland mantle plume. *Nature* 385, 245–247.
- Woodhouse, J.H., Dziewonski, A.M., 1984. Mapping the upper mantle: three-dimensional modeling of earth structure by inversion of seismic waveforms. *J. Geophys. Res.* 89, 5953–5986.
- Yegorova, T.P., Kozlenko, V.G., Pavlenkova, N.I., Starostenko, V.I., 1995. 3-D density model for the lithosphere of Europe: construction method and preliminary results. *Geophys. J. Int.* 121, 873–892.